I.G. GRAHAM, W. HACKBUSCH AND S.A. SAUTER

Hybrid Galerkin Boundary Elements on Degenerate Meshes

1. Introduction

In recent work ([4],[5]) the authors have presented a new discretisation scheme for boundary integral equations which has the same energy norm stability and convergence properties as the Galerkin method but has a complexity comparable with discrete collocation or Nyström methods. The results in [4],[5] were for non-quasiuniform but nevertheless shape-regular meshes. Here we extend the theory to much more general meshes, including the degenerate meshes commonly used to handle singularities arising from corners and edges in 3D applications. As an application we give numerical results for the classical problem of computing the capacitance of a two-dimensional plate in $\mathbb{R}^3$. These show that the method is capable of attaining the same type of complexity reduction for singular problems as was already attained for smooth applications in [5].

Our new method is an approximate Galerkin method, where the integrals arising in the matrix are computed by quadrature. The important novel feature is that the matrix is (adaptively) partitioned into (i) a small "conventional Galerkin" part (near the diagonal), in which standard triangle-based quadrature rules are used to compute the singular or nearly singular integrals, and (ii) the remainder, which is done by novel node-based rules. In effect, in (ii), suitable approximations to the Galerkin matrix entries are computed from local weighted averages of elements of the "Nyström matrix" (formed from kernel evaluations only at nodal points of the mesh). This has a low complexity compared with the method in (i), since triangle-based rules typically use (often many) additional kernel evaluations at non-nodal points. The ability of the new method to compute most of the matrix using the cheaper method is the key to its competitiveness. The term "*hybrid*" is used because, in a certain way, the new method is a blend of two classical methods: Galerkin and Nyström. We note that the word "hybrid" is also used to describe various other methods, but, as far as we are aware, these have no connection with the "hybrid Galerkin method" proposed here.

Nevertheless we want to mention here that our work has connections to two earlier works [12, 1]. In particular [12], considers 2D boundary integral equations with operator composed of the sum of a convolution and a (smooth) compact perturbation. The convolution part is discretised by the Galerkin method, yielding a Toeplitz matrix which can be assembled very efficiently in a semi-discrete manner ([12, p.257]). The smooth perturbation and the the right-hand side function are discretised by node-based quadrature analogous to that proposed below. In a different but related direction, [1] proves stability for nodal collocation onto splines of odd degree (again for integral equations on 2D contours) by utilising a discrete integration by parts argument to show that the collocation equations are equaivalent to a non-standard Galerkin method. Thus [1] utilises the link between the discrete Galerkin and collocation methods. We also exploit this link, but our method considers in fact fully discrete quadrature errors and more precisely exploits an analogous link between the discrete Galerkin and Nyström methods. In addition our work concerns integral equations on 3D surfaces.

This work was supported by British Council / DAAD ARC Grant 869.

Thus, in general we shall consider (first or second kind) integral equations of the form

$$(\lambda I + \mathcal{K})u(\mathbf{x}) := \lambda u(\mathbf{x}) + \int_\Gamma k(\mathbf{x},\mathbf{y})u(\mathbf{y})dy = f(\mathbf{x}), \quad \mathbf{x} \in \Gamma , \tag{1}$$

where $\lambda \in \mathbb{R}$, $\Gamma = \cup\{\overline{\Gamma}_\ell : \ell = 1, \ldots, L\}$ is the surface of a polyhedron in $\mathbb{R}^3$ with (open) polygonal faces Γ_ℓ. (The method and analysis given here extends to general piecewise smooth (curved) Lipschitz surfaces - as described in the case of non-degenerate meshes in [4, 5] - but for brevity's sake (only), we do not give that generality here.)

For (1), we assume that for some $\mu \in [-1, 1]$, $\lambda I + \mathcal{K} : H^\mu \to H^{-\mu}$. We also assume that the bilinear form $a(u, v) := ((\lambda I + \mathcal{K})u, v)$ is elliptic in H^μ and that $f \in H^{-\mu}$. (Here $(\cdot,\cdot)$ denotes the usual L_2 inner product on Γ.) Finally we assume also that the kernel k has the characteristic singularity which arises in fundamental solutions of elliptic PDEs (or derivatives of fundamental solutions), i.e., for some $\alpha \in \mathbb{R}$ and all $m \in \mathbb{N}_0$, $|D^m k(\mathbf{x},\mathbf{y})| \le B_m|\mathbf{x}-\mathbf{y}|^{-\alpha-m}$ holds, where B_m is a constant and D^m denotes any mth order partial differential operator with respect to $(\mathbf{x},\mathbf{y}) \in \Gamma_\ell \times \Gamma_{\ell'}$. Note that this ensures that $k \in \mathcal{C}^\infty(\Gamma_\ell \times \Gamma_{\ell'})$ when $\ell \neq \ell'$, but it allows k to be discontinuous across the edges of Γ (as happens, for example, with the double layer potential kernel).

2. Discrete Galerkin Methods

The main object of this paper is to extend the theoretical results of [4, 5] to more general (irregular) mesh sequences, including the anisotropic graded meshes typically used to handle edge and corner singularities.

We want to emphasise that the hybrid Galerkin method proposed here can in practice be applied directly to general boundary integral equations on curved surfaces, discretised using discontinuous or continuous elements on triangular or quadrilateral meshes. For illustrative purposes we restrict here to the model case of piecewise flat surfaces and continuous linear triangular elements. More general theory is given in [4, 5] and further extensions will be addressed in a fourthcoming paper.

For the approximation of (1), we introduce a family of triangular meshes $\mathcal{T}_h$ $(h \to 0)$ on Γ, each of which consists of open planar triangles $\tau \in \mathcal{T}_h$. (We assume that the edges of Γ consist of triangle edges.) The nodes of $\mathcal{T}_h$ are denoted $\{\mathbf{x}_p : p \in \mathcal{N}\}$, with $\mathcal{N}$ denoting a suitable index set. We set $N = \#\mathcal{N}$. For any $\tau \in \mathcal{T}_h$, we let $|\tau|$ denote its area, h_τ its diameter and r_τ its smallest perpendicular height:

$$r_\tau = 2|\tau|/h_\tau \tag{2}$$

For $p \in \mathcal{N}$, $\mathcal{T}_h(p) := \{\tau \in \mathcal{T}_h : \mathbf{x}_p \in \overline{\tau}\}$. The parameter h is identified with the maximum mesh diameter: $h = \sup\{h_\tau : \tau \in \mathcal{T}_h\}$. We also introduce the "local mesh diameters": $h_p = \max\{h_\tau : \tau \in \mathcal{T}_h(p)\}$. As in [4], if A and B are any two quantities which depend (implicitly or explicitly) on h, we use the notation $A \lesssim B$ to mean that $A \le const B$, with *const* denoting a constant independent of h.

The chief new theoretical contribution of this paper is to develop the theory of hybrid Galerkin methods for meshes which satisfy only very weak regularity assumptions as $h \to 0$. Specifically we require (with *l.q.u.* an abbreviation for *locally quasiuniform*):

(**A1**) The number of triangles adjoining any node is bounded: $\max_{p\in\mathcal{N}}\{\#\mathcal{T}_h(p)\} \lesssim 1$.

(**A2**) The triangle areas are *l.q.u.*: $\max_{p\in\mathcal{N}} \max_{\tau,\tau'\in\mathcal{T}_h(p)}\{|\tau|/|\tau'|\} \lesssim 1$.

(**A3**) The minimal heights are *l.q.u.*: $\max_{p\in\mathcal{N}} \max_{\tau,\tau'\in\mathcal{T}_h(p)}\{r_\tau/r_{\tau'}\} \lesssim 1$.

It is easy to show (see, e.g. [4, §2.5]) that shape-regular meshes satisfy (**A1**)-(**A3**). However more general meshes are also allowed, in particular the degenerate meshes which result from anisotropic algebraic or geometric refinement used (respectively) in the $h-$ or $hp-$approximations of solutions with edge singularities (e.g. [7, 3, 10]). Using these meshes, we define $\mathcal{S}_h$ to be the space of continuous piecewise linear functions on Γ with respect to $\mathcal{T}_h$, spanned by the usual basis $\{\phi_p : p \in \mathcal{N}\}$ with $\phi_p(\mathbf{x}_q) = \delta_{p,q}$, for all $p, q \in \mathcal{N}$.

The *Galerkin method* for (1) seeks $U \in \mathcal{S}_h$ such that

$$a(U, V) = (f, V), \quad \text{for all } \; V \in \mathcal{S}_h \; , \tag{3}$$

With the expansions $U = \sum_{q\in\mathcal{N}} U_q\phi_q$ and $V = \sum_{p\in\mathcal{N}} V_p\phi_p$, we have

$$a(U, V) = \sum_{p\in\mathcal{N}}\sum_{q\in\mathcal{N}} U_q(\lambda M_{p,q} + K_{p,q})V_p \; , \tag{4}$$

where $M_{p,q} = (\phi_q, \phi_p)$ and

$$K_{p,q} = (\mathcal{K}\phi_q, \phi_p) = \int_\Gamma\int_\Gamma k(\mathbf{x}, \mathbf{y})\phi_q(\mathbf{y})\phi_p(\mathbf{x})dydx \; , \tag{5}$$

The exact Galerkin method (3) reduces to the solution of a linear system with coefficient matrix $(\lambda M_{p,q} + K_{p,q})_{p,q\in\mathcal{N}}$.

Discrete Galerkin methods arise when the matrix elements are approximated by quadrature. The (sparse) M is relatively trivial to compute, but in almost all 3D engineering applications it is necessary to approximate K by quadrature. In general we let $\tilde{a}$ denote the result of replacing $K_{p,q}$ in (4) by some approximation $\tilde{K}_{p,q}$:

$$\tilde{a}(U, V) = \sum_{p\in\mathcal{N}}\sum_{q\in\mathcal{N}} U_q(\lambda M_{p,q} + \tilde{K}_{p,q})V_p \; . \tag{6}$$

Then the corresponding *discrete Galerkin* solution $\tilde{U}$ is defined to be the solution of (3) with a is replaced by $\tilde{a}$. (Related semidiscrete methods are discussed in [11].)

To define suitable $\tilde{K}_{p,q}$, let us first restrict attention to the (most common) case when $\mathrm{supp}\phi_p \cap \mathrm{supp}\phi_q = \emptyset$. Then in (5) the kernel k is smooth on each of the faces of Γ but may be discontinuous across edges. We shall build approximations to $K_{p,q}$ from fundamental quadrature rules of the form:

$$\int_\Gamma F\phi_p \approx \sum_{j\in J_p} w_j F(\mathbf{z}_j) \; , \quad \text{for each } p \in \mathcal{N} \; . \tag{7}$$

Here J_p is a finite index set, w_j are weights and $\mathbf{z}_j$ are quadrature points on Γ which are "near" supp ϕ_p. The integral (5) can then be computed by applying such rules for the integrals over $\mathbf{x}$ and $\mathbf{y}$, yielding

$$\tilde{K}_{p,q} = \sum_{j \in J_p} \sum_{j' \in J_q} w_j k(\mathbf{z}_j, \mathbf{z}_{j'}) w_{j'} \ . \tag{8}$$

Because of the regularity of k, (7) has to make sense for functions F which are discontinuous across edges of Γ. When any $\mathbf{z}_j$ lies on such an edge, the notation $F(\mathbf{z}_j)$ in (7) should be understood as an abbreviation for the *limit* of $F(\mathbf{x})$ as $\mathbf{x} \to \mathbf{z}_j$ from within *one* particular face of Γ. With this convention the quantity $F(\mathbf{z}_j)$ may appear more than once in (7), but with different weights according to which face the limiting value is taken from. The implicit notation (7) is sufficient for theoretical purposes. More precise practical details are given in [4].

Let $\mathcal{P}_d(\Gamma)$ denote the discontinuous functions on Γ which reduce to bivariate polynomials of degree d on each of the faces Γ_ℓ. Then we will be interested in rules (7) which satisfy the assumptions (for some $d \in \mathbb{N}_0$ and $\sigma,\ \delta \geq 1$ independent of h):

(**A4**) *"Degree of Precision"*: Equality holds in (7) for all $F \in \mathcal{P}_d(\Gamma)$;

(**A5**) *"Stability"*: $\sum_{j \in J_p} |w_j| \leq \sigma \sum_{j \in J_p} w_j$, for all p ;

(**A6**) *"Compactness"*: $\sup_{j \in J_p} |\mathbf{z}_j - \mathbf{x}_p| \leq \delta h_p$, for all p .

Examples of rules satisfying (**A4**) - (**A6**) for any $d \in \mathbb{N}$, with $\sigma = \delta = 1$ are furnished by separating the left-hand side of (7) into a sum of integrals over the triangles $\tau \in \mathcal{T}_h(p)$ and then applying suitable rules to integrate $F\phi_p$ over triangles. An alternative (with reduced complexity, as mentioned above), is to construct (7) using only quadrature points chosen exclusively from the set of nodal points $\{\mathbf{x}_p : p \in \mathcal{N}\}$ of the mesh and which have the exactness property (**A4**) for some required d.

To see how to do this, suppose, for example, that supp ϕ_p lies entirely within one $\overline{\Gamma}_\ell$. Then to achieve (**A4**) for $d = 1$ we would choose 3 nodes $\{\mathbf{x}_j\}$ near $\mathbf{x}_p$ and require (7) to hold for all functions F which are polynomials of degree 1 on Γ_ℓ. This leads to a 3×3 system to be solved for the weights w_j. Increasing d leads to larger systems for the weights but, for any fixed d, the cost of doing this for all $p \in \mathcal{N}$ is still only $O(N)$. For these "node-based" rules, assumptions (**A4**), (**A6**) can in principle be satisfied directly by construction, but nonsingularity of the systems to be solved for the weights (and the consequent size of the stability constant σ) is, in general, unknown *a priori*. In [5] (see also §5 below), we give a very detailed theory on this question, which shows that for $d \leq 2$, all "reasonable" choices of quadrature points lead to a stability constant σ which is bounded independently of h.

Remark 1. If supp ϕ_p does not lie entirely within one face of Γ then it will be necessary to split the support up into components belonging to each of the smooth faces and construct appropriate quadrature rules on each face (see also [4]).

It should now be clear why the use of node-based rules can decrease the complexity of computing the matrix K: If kernel evaluations within triangles are used then this will automatically be more expensive than methods which confine the evaluations to the nodes and in many cases a reduction in kernel evaluations by a factor of between

10 and 70 is possible using node-based rules (see [5]). (For quadrilateral elements the same principle applies, although the complexity achievable depends on the individual choices of quadrature rules.)

So far we have not discussed the fundamental question of how the degree of precision of the rules used for computing each $K_{p,q}$ should be chosen in order to preserve the optimal order of convergence of the underlying Galerkin method. We show below that in order to achieve this, d needs only to be quite low (e.g. 1 or 2) in the "far field" (where $\mathbf{x}_p$ and $\mathbf{x}_q$ are well-separated), and d needs to increase modestly as the distance between $\mathbf{x}_p$ and $\mathbf{x}_q$ decreases. In the *singular case* supp $\phi_p \cap$ supp $\phi_q \neq \emptyset$, regularising transforms and triangle-based rules must be used [8, 10]. We now give an algorithm in which efficient quadrature rules which maintain optimal convergence rates are determined automatically. It has a first phase in which node-based rules satisfying (**A1**)-(**A3**) for some (small) choices of d are computed. Then in the second phase these are used to compute (5), provided this integral is sufficiently far from being singular. In determining what degree of precision should be employed the following quantities are useful: $h_{p,q} := \max\{h_p, h_q\}$, and

$$\rho_{p,q} = \min\{|\mathbf{x} - \mathbf{y}| : \mathbf{x} \in \text{supp } \phi_p \cup \{\mathbf{z}_j : j \in J_p\},\ \mathbf{y} \in \text{supp } \phi_q \cup \{\mathbf{z}_{j'} : j' \in J_q\}\} \ .$$

The algorithm requires the user to choose the following parameters: real numbers $\delta, \sigma, C^* \geq 1$ and positive integers $d_{\min} \leq d_{\max}$. Also set $\chi = 1 - \mu - \min\{\mu, 0\}$, where μ is as defined in §1.

Hybrid Galerkin Algorithm

procedure generate_node_based_quadrature_rules;
begin
  for all $p \in \mathcal{N}$ **do**
    for all integers $d \in [d_{\min}, d_{\max}]$ **do**
    (i) Select $(d+1)(d+2)/2$ nodes $\{\mathbf{x}_j : j \in J_p = J_p(d)\}$ on Γ near $\mathbf{x}_p$.
    (ii) Find $\{w_j : j \in J_p(d)\}$ such that (7) is exact for polynomials F of degree d.
    (iii) If the w_j satisfy (**A5**),(**A6**):
      set $B_p(d) =$ "admissible" and store the $J_p(d)$ and w_j.
    (iv) If the w_j do not satisfy (**A5**),(**A6**), set $B_p(d) =$ "inadmissible".
    end of loop over d
  end of loop over p
end;

Remark 2. If $\mathbf{x}_p$ is an edge node of Γ, the procedure above must be slightly modified (see Remark 1).

Remark 3. Step (ii) requires solution of a square system. It is also permissible to select more than $(d+1)(d+2)/2$ quadrature points, provided the resulting underdetermined system is solved by a minimal norm algorithm [5, §3.3].

The second phase of the algorithm then follows:

procedure generate_hybrid_system_matrix;
begin
for all $p, q \in \mathcal{N}$ **do**
begin

- Compute d_{pq}, the smallest positive integer satisfying

$$d_{p,q} \geq \frac{\chi + (1+\alpha)\log(C^*\rho_{p,q})/\log h_{p,q}}{1 - \log(C^*\rho_{p,q})/\log h_{p,q}} \tag{9}$$

if ($d_{p,q} \in [d_{\min}, d_{\max}]$) and ($B_p(d_{pq})$ = "admissible") and ($B_q(d_{pq})$ = "admissible") **then**

- Compute $\tilde{K}_{pq}$ using the node-based rules obtained above.

else

- Compute $\tilde{K}_{pq}$ using triangle-based rules, and ensure that

$$|K_{p,q} - \tilde{K}_{p,q}| \leq C h_{p,q}^{\chi+1} s_p s_q \ . \tag{10}$$

end
end;

Remark 4. (10) is always possible, with C independent of h, using triangle-based rules (see [2, 8, 10]).

In the next section we prove the stability and convergence of this algorithm.

3. Convergence Theory

Since Galerkin stability follows from the continuity and ellipticity of a, discrete Galerkin stability can be obtained using the "Strang Lemma", provided the error $a - \tilde{a}$ is suitably small on $\mathcal{S}_h \times \mathcal{S}_h$. The estimation of this error often makes use of *inverse inequalities* (especially when $\mu < 0$) and for these, the meshes normally need to be quasiuniform. However in [4, §3] we obtained more general norm inequalities which play the role of inverse estimates in the theory but which hold true for meshes assumed only to be shape-regular. It turns out that these norm inequalities can be further generalised to include degenerate meshes and the results are as follows.

Recalling (2), we define, for $p \in \mathcal{N}$, $s_p = \int_\Gamma \phi_p = \sum_{\tau \in \mathcal{T}_h(p)} |\tau|/3$ and $r_p = \max\{r_\tau : \tau \in \mathcal{T}_h(p)\}$. Then, for any $t \in \mathbb{R}$, define the weighted ℓ_2-norms $\|\cdot\|_{\ell_2,t}$ by:

$$\|\boldsymbol{V}\|_{\ell_2,t}^2 = \sum_{p \in \mathcal{N}} r_p^{2t} s_p |V_p|^2 \ , \quad \boldsymbol{V} = (V_p)_{p \in \mathcal{N}} \in \mathbb{R}^N \ .$$

We also define $\mathcal{I} : \mathbb{R}^N \to \mathcal{S}_h$, by: $\mathcal{I}\boldsymbol{V} = \sum_{p \in \mathcal{N}} V_p \phi_p$. The following result is a generalisation of [4, Theorem 3.5]. Its proof will be given in a fourthcoming paper.

Theorem 1 *For all* $t \in [0,1]$ *and* $\boldsymbol{V} \in \mathbb{R}^N$*,*

$$\|\boldsymbol{V}\|_{\ell_2,t} \lesssim \|\mathcal{I}\boldsymbol{V}\|_{H^{-t}} \lesssim \|\boldsymbol{V}\|_{\ell_2,0} \lesssim \|\mathcal{I}\boldsymbol{V}\|_{H^t} \lesssim \|\boldsymbol{V}\|_{\ell_2,-t} \ .$$

From this we can prove the following result, which estimates the error $a - \tilde{a}$ in the form required by the Strang Lemma.

Theorem 2 *Let $\tilde{K}$ be obtained by the hybrid Galerkin algorithm and define $\tilde{a}$ by (6). Suppose $h < 1$, $t \in [-1, 1]$ and set $t^* = \min\{t, 0\}$. Then*

$$\frac{|a(V,W) - \tilde{a}(V,W)|}{\|V\|_{H^t} \|W\|_{H^t}} \lesssim Ch^{\chi+1} \sum_{\tau \in \mathcal{T}_h} h_\tau^{-2t^\star} |\tau|^{1+2t^\star} \tag{11}$$

$$\frac{|a(V,W) - \tilde{a}(V,W)|}{\|V\|_{H^0} \|W\|_{H^t}} \lesssim Ch^{\chi+1} \left\{ \sum_{\tau \in \mathcal{T}_h} h_\tau^{-2t^\star} |\tau|^{1+2t^\star} \right\}^{1/2}, \tag{12}$$

with C denoting a generic constant which depends on C^*, δ and σ.

Proof. We start by estimating the errors $|K_{pq} - \widetilde{K}_{pq}|$. First, if $\widetilde{K}_{pq}$ is computed by a node-based rule with degree of precision d_{pq}, then $B_p(d_{pq}) = B_q(d_{pq}) =$ "admissible", $d_{p,q}$ satisfies (9) and $d_{p,q} \in [d_{\min}, d_{\max}]$. From these it follows that $\log(C^\star \rho_{p,q}) / \log h_{p,q} < 1$. Then, since $h_{p,q} \le h < 1$, a simple rearrangement of (9) shows that

$$\rho_{p,q} \ge (C^*)^{-1} h_{p,q}^{(d_{p,q}-\chi)/(d_{p,q}+1+\alpha)}. \tag{13}$$

Now, a careful examination of the arguments in [4] shows that [4, Lemma 4.3], remains true even for the more general meshes satisfying (**A1**) - (**A3**), i.e., there exists $C = C(\delta, \sigma)$ such that

$$|K_{p,q} - \tilde{K}_{p,q}| \le Ch_{p,q}^{d_{p,q}+1} \rho_{p,q}^{-(d_{p,q}+1+\alpha)} s_p s_q. \tag{14}$$

Combining (14) with a simple rearrangement of (13) yields

$$\left| K_{pq} - \widetilde{K}_{pq} \right| \le Ch_{p,q}^{\chi+1} s_p s_q. \tag{15}$$

In fact (15) holds even when triangle-based rules are used because of the explicit condition (10).

Now we can proceed with the proofs of (11), (12). First observe that by (15),

$$\begin{aligned} |a(V,W) - \tilde{a}(V,W)| &\le \sum_{p,q \in \mathcal{N}} |V_q||K_{p,q} - \tilde{K}_{p,q}||W_p| \\ &\lesssim Ch^{\chi+1} \sum_{q \in \mathcal{N}} s_q |V_q| \sum_{p \in \mathcal{N}} s_p |W_p|. \end{aligned} \tag{16}$$

To bound (16), observe that, for any $t \in [-1, 1]$ and $t^\star = \min\{t, 0\}$, we have, using Cauchy-Schwarz and Theorem 1,

$$\begin{aligned} &\sum_{p \in \mathcal{N}} s_p |W_p| = \sum_{p \in \mathcal{N}} r_p^{-t^\star} s_p^{1/2} |W_p| r_p^{t^\star} s_p^{1/2} \\ &\lesssim \left\{ \sum_{p \in \mathcal{N}} r_p^{-2t^\star} s_p |W_p|^2 \right\}^{1/2} \left\{ \sum_{p \in \mathcal{N}} r_p^{2t^\star} s_p \right\}^{1/2} \lesssim \left\{ \sum_{p \in \mathcal{N}} r_p^{2t^\star} s_p \right\}^{1/2} \|W\|_{H^{t^\star}}. \end{aligned} \tag{17}$$

Now note that, by definition of r_p, we have $r_p^{2t^*} \le r_{\tau'}^{2t^*}$ for all $\tau' \in \mathcal{T}_h(p)$. Hence, using (**A3**), we have

$$r_p^{2t^*} s_p \le r_{\tau'}^{2t^*} \sum_{\tau \in \mathcal{T}_h(p)} |\tau|/3 \lesssim \sum_{\tau \in \mathcal{T}_h(p)} r_\tau^{2t^*} |\tau|.$$

Now, using the definition of r_τ (2), it follows that

$$\sum_{p\in\mathcal{N}} r_p^{2t^*} s_p \lesssim \sum_{p\in\mathcal{N}} \sum_{\tau\in\mathcal{T}_h(p)} h_\tau^{-2t^*} |\tau|^{1+2t^*} \ . \tag{18}$$

Now substitution of (18) into (17) and noting that $\|V\|_{H^{t^\star}} \le \|V\|_{H^t}$, yields

$$\sum_{p\in\mathcal{N}} s_p|W_p| \lesssim \left\{\sum_{\tau\in\mathcal{T}_h} h_\tau^{-2t^\star} |\tau|^{1+2t^\star}\right\}^{1/2} \|W\|_{H^t} \, . \tag{19}$$

Using (19) twice in (16) yields (11). Also, since (19) holds for any t and W we have, in particular,

$$\sum_{q\in\mathcal{N}} \int \phi_q \, |V_q| \lesssim \left\{\sum_{\tau\in\mathcal{T}_h} |\tau|\right\}^{1/2} \|V\|_{H^0} \lesssim \|V\|_{H^0} \, . \tag{20}$$

Combining (19), (20) with (16) yields (10).

Combining the result of Theorem 2 with the Strang Lemma (e.g. [4]) we have
Corollary 3 *Let $\mu^* = \min\{\mu, 0\}$. If the mesh sequence $\mathcal{T}_h$ satisfies*

$$h^{\chi+1} \sum_{\tau\in\mathcal{T}_h} h_\tau^{-2\mu^\star} |\tau|^{1+2\mu^\star} \to 0 \ , \quad \text{as} \ \ h \to 0 \ , \tag{21}$$

then the hybrid Galerkin solution $\tilde{U}$ is stable and satisfies the error bound:

$$\left\|u - \tilde{U}\right\|_{H^\mu} \lesssim \inf_{V\in S_h} \left\{ \|v - V\|_{H^\mu} + h^{\chi+1} \left\{\sum_{\tau\in\mathcal{T}_h} h_\tau^{-2\mu^\star} |\tau|^{1+2\mu^\star}\right\}^{1/2} \right\} . \tag{22}$$

Remark 5. Recalling that $\chi = 1-\mu-\mu^*$, it is easy to see that the stability condition (21) is automatically satisfied when $\mu = 0$ or $\mu = 1/2$ (double layer or hypersingular operator arising from the Laplacian), and that the stability condition when $\mu = -1/2$ (single layer) is $h^3 \sum_{\tau\in\mathcal{T}_h} h_\tau \to 0$. This is a very mild condition. Indeed we shall see in the next section that it is satisfied for strongly anisotropic meshes, and indeed the error estimate (22) turns out to be optimal in this case.

4. Numerical Experiment: Capacitance of a plate

In this section we report on some numerical experiments for the hybrid Galerkin algorithm applied to the single layer potential equation:

$$\mathcal{K}u(\mathbf{x}) := -\frac{1}{4\pi} \int_\Gamma \frac{1}{|\mathbf{x}-\mathbf{y}|} u(\mathbf{y}) dy = f(\mathbf{x}) \ , \ \ \mathbf{x} \in \Gamma \ , \tag{23}$$

where $\Gamma = \{(x_1, x_2, 0)^T : x_1, x_2 \in [0,1]\}$ is the two-dimensional unit square in $\mathbb{R}^3$. We will be concerned with the special case $f \equiv 1$, in which case the capacitance κ of the plate is given by the formula:

$$\kappa = -\frac{1}{4\pi} \int_\Gamma u(\mathbf{x}) dx \ . \tag{24}$$

(See also [11].) For this problem the parameters μ (the Sobolev index of the energy norm) and α (the rate of blow-up of the kernel) are $-1/2$ and 1, respectively.

It is known that the solution u of this problem has corner and edge singularities. In fact, as $\mathbf{x} \in \Gamma$ approaches an interior point $\mathbf{x}_0$ of an edge (in the normal direction), then $u(\mathbf{x}) = O(|\mathbf{x} - \mathbf{x}_0|^{-1/2})$. (This edge singularity is more severe than any arising from problem (23), when Γ is any (closed) Lipschitz polyhedron - see, e.g., [7]. The optimal approximation of these singularities can be obtained only by appropriate mesh refinement near the edges of Γ. This may be implemented either *adaptively* or *a priori*. In this experiment we shall implement a sequence of *a priori* graded meshes which yield optimal approximations for this problem, with a complexity (in terms of numbers of degrees of freedom) which is the same as that of uniform meshes. This low complexity arises because the meshes are strongly *anisotropic* i.e., near the interior portions of edges they are highly refined in the direction orthogonal to the edge, but are more or less uniformly subdivided in the direction tangential to the edges. To define these meshes, for each integer $n \geq 1$, and a *grading exponent* $g \geq 1$, we introduce the points in $[0,1]$: $t_i = (i/n)^g/2$, and $t_{2n-i} = 1 - (i/n)^g/2$, for $i = 0, \ldots, n$. Then, for $i, j = 1, \ldots 2n+1$, we introduce the nodes of the tensor-product mesh on Γ: $\mathbf{x}_{i,j} = (t_i, t_j)^T$. From these we construct a triangular mesh by dividing each of the rectangles into two using its diagonal (drawn from bottom left to top right). As g increases these 2D meshes become more anisotropic, with the most extreme triangles having an aspect ratio of about gn^{g-1}. Nevertheless these meshes satisfy assumptions (**A1**)-(**A3**) above. In [7] it was shown that if $\mathcal{S}_n$ denotes the discontinuous piecewise linear basis functions defined on these meshes, then there exists $\xi_n \in \mathcal{S}_n$ such that $\|U - \xi_n\|_{-1/2} \leq C(1/n)^{\min(g-\epsilon,5)/2}$ (for arbitrary $\epsilon > 0$). In addition, in [3] it is shown that if U_n denotes the Galerkin solution to (23) in any subspace of $H^{-1/2}$, and if κ_n denotes the corresponding approximation to the capacitance obtained by substituting U_n into (24), then $|\kappa - \kappa_n| \leq C\|u - U_n\|^2_{-1/2}$. Combining these two inequalities, we expect that with discontinuous piecewise linear basis functions,

$$|\kappa - \kappa_n| \leq C(1/n)^{\min(g-\epsilon,5)} \ , \quad \text{for} \quad g \geq 1 \text{ and } \epsilon > 0. \tag{25}$$

Since the space of continuous piecewise linear functions is contained in the space of discontinuous piecewise linears we cannot expect a better rate than (25) for our discretisation. Our experiments indicate that (25) remains true in the discontinuous case. Assuming this, since $\mu = \mu^* = -1/2$ and $\chi = 2$, the second term on the right hand side of (22) can be shown to be $O(1/n)^{5/2}$ and condition (21) holds. Then. by Corollary 3, $\|u - \tilde{U}\|_{-1/2} = O(1/n)^{5/2}$ and so the capacitance $\tilde{\kappa}_n$ obtained by inserting the hybrid Galerkin solution $\tilde{U}$ into (24) also satisfies (25). Our experiments also indicate this to be true.

In the following experiments we implement the hybrid Galerkin algorithm with parameter choice and $d_{\min} = d_{\max} = 2$ and various C^*. For this choice of parameters the right-hand side of (9) is bounded above by 2 (as $n \to \infty$) for p, q satisfying

$$\rho_{p,q} \geq 1/C^* \ . \tag{26}$$

Thus in our experiments the condition (9) is replaced by (26), i.e. node-based rules are used only for p, q satisfying (26).

In the most general version of the hybrid algorithm the parameters δ and σ in (**A5**), (**A6**) depend upon the choice of points in the node-based rules. In these experiments we choose quadrature points around each node (depicted below) which satisfy (**A6**) for $\delta = 2$. Moreover the theory in [5] can be used to show that for our choices of quadrature points, (**A5**) holds with σ independent of n (but dependent on g). We choose here not to stipulate in advance an upper bound for σ but rather we run the code and record the computed smallest value of σ for which (**A5**) holds.

To construct node-based quadrature rules of degree of precision 2 we need to choose at least 6 nodes near the reference node $\mathbf{x}_p$. In fact, for all nodes except the four corner nodes, we chose 7 nodes and computed the weights using a minimal norm method for underdetermined systems (see [5]). The choices of nodes used is given diagrammatically below. In each picture the circled dot denotes $\mathbf{x}_p$ and the other dots denote the nodes which (together with $\mathbf{x}_p$) are used to compute a rule of precision 2.

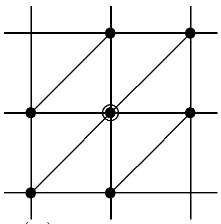

(a) Interior node

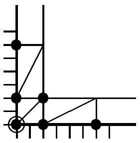

(b) Corner node

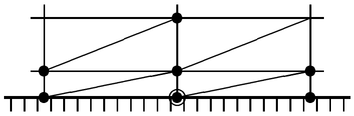

(c) Edge node

Finally, to fully describe the algorithm which we have implemented we must stipulate how we have computed the triangle-based Galerkin integrals in the "near field" when (26) does not hold. To do this we take the double integral (5) and expand it in the conventional way as a double sum of integrals over pairs of triangles in supp $\phi_p \times$ supp ϕ_q. For pairs of triangles which touch we use the regularising transformations in [2] to reduce these to smooth integrals over tensor products of a simplex in $\mathbb{R}^s$ and $[0,1]^{4-s}$, $s = 1, 2, 3$. The resulting integrals are computed using conical Gauss rules. For pairs of triangles which do not touch (but for which (26) does not hold), we use again conical Gauss rules in each triangle. The numbers of points in these Gauss rules were adjusted experimentally until we were confident that the corresponding Galerkin integrals were accurate to 5 figures. For triangles which have high aspect ratio, it was found necessary to choose highly accurate Gaussian rules in order to preserve the overall convergence of the method. In particular for pairs of triangles which touch, we chose the degree of precision increasing approximately linearly with the maximum of the aspect ratios of the pair. (For example, in Table 1 for $N = 169$, integrals over the most distorted intersecting triangles required up to 14 Gauss points in some coordinate directions.) A similar increase in precision was necessary for disjoint pairs of triangles whose distance apart was smaller than the maximum of the diameters of each of the triangles in the pair. In [3] a semi-analytic method was used for computing the Galerkin matrix, and so these difficulites could be somewhat reduced. (See also [11].) However in more general cases, fully discrete quadrature can not be avoided and so the experiments recorded here provide a guide to what may happen in larger applications.

In the tables presented below we use the following notation: $N = (2n+1)^2$ denotes the number of nodes in the mesh, σ denotes the computed stability constant in (**A5**), $\tilde{\kappa}_n$ denotes the capacitance computed using the hybrid algorithm and the column headed % denotes the percentage of the matrix entries which were computed using the node-based rules. Table 1 gives results for $g = 3$ in the "true Galerkin" case where $C^* = 0.5$ $(< \mathrm{diam}(\Gamma))^{-1}$. By (26), no entries of the matrix are computed with node-based rules. Based on (25) we expect $\tilde{\kappa}_n$ to converge with about $O(1/n)^3$ to κ. From this, extrapolation yields a true value $\kappa \cong 0.73363$, which coincides to 4 decimal places with the suggested true value in [3]. We use this to compute the errors and the estimated order of convergence (EOC). Table 2 repeats this experiment for $C^* = 2, 4$. As C^* increases a higher percentage of the matrix is computed using node-based rules. For $C^* = 2$ the asymptotic convergence rate predicted in (25) is clearly visible. This is less clear for the case $C^* = 4$, where finer meshes will be required before asymptotia is reached. This observation resonates with the theory, since the constant C in (14) is known to grow as C^* increases (see also [5, eq. (2.16)]). For $N = 169$ and $C^* = 2$, more than half the matrix is computed with a node-based rule of precision 2. Thus uses about 64 times fewer kernel evaluations than the cheapest triangle-based rules used in Table 1, but the increase in error is only 9×10^{-5}. To further illustrate the effect of the grading exponent g, we repeat this experiment with a uniform mesh $g = 1$. In Table 3 a convergence rate of only $O(1/n)$ is observed, but with a remarkably robust dependence on C^*.

N	$\tilde{\kappa}_n$	$\lvert\kappa - \tilde{\kappa}_n\rvert$	EOC	%
25	0.729115	4.5(-3)	2.7	0
49	0.732154	1.5(-3)	2.3	0
81	0.732848	7.8(-4)	3.3	0
121	0.733257	3.7(-4)	1.7	0
169	0.733364	2.7(-4)	3.0	0
225	0.733461	1.7(-4)		0

Table 1: $q = 3,\ C^* = 0.5$

		$C^* = 2$				$C^* = 4$			
N	σ	$\tilde{\kappa}_n$	$\lvert\kappa - \tilde{\kappa}_n\rvert$	EOC	%	$\tilde{\kappa}_n$	$\lvert\kappa - \tilde{\kappa}_n\rvert$	EOC	%
25	5.7	0.729129	4.5(-3)	2.7	9	0.729047	4.6(-3)	2.2	24
49	5.7	0.732168	1.5(-3)	2.2	34	0.731726	1.9(-3)	1.9	56
81	4.0	0.732835	8.0(-4)	2.5	44	0.732516	1.1(-3)	3.2	62
121	4.0	0.733167	4.6(-4)	3.1	49	0.733093	5.4(-4)	1.4	65
169	4.0	0.733375	2.6(-4)		53	0.733215	4.2(-4)		71

Table 2: $q = 3,\ C^* = 2, 4$

		$C^*=2$				$C^*=4$			
N	σ	$\tilde{\kappa}_n$	$\|\kappa-\tilde{\kappa}_n\|$	EOC	%	$\tilde{\kappa}_n$	$\|\kappa-\tilde{\kappa}_n\|$	EOC	%
25	2.0	0.718333	1.5(-2)	0.8	4	0.718833	1.5(-2)	1.0	30
49	2.0	0.723048	1.1(-2)	1.1	7	0.723221	1.0(-2)	0.7	37
81	2.0	0.725532	8.1(-3)	0.9	25	0.725580	8.1(-3)	1.0	59
121	2.0	0.727056	6.6(-3)	0.9	29	0.727127	6.5(-3)	0.9	59
169	2.0	0.728077	5.6(-3)		33	0.728083	5.5(-3)		66

Table 3: $q=1,\ C^*=2,4$

References

[1] D.N. Arnold and W.L. Wendland, On the asymptotic convergence of collocation methods, Math. Comp. **41**, 349–381, 1983.

[2] S. Erichsen and S. A. Sauter. Efficient automatic quadrature in 3D Galerkin BEM. To appear in Comp. Meth. Appl. Mech. Eng., 1998.

[3] V.J. Ervin, E.P. Stephan and S. Abou El-Seoud, An improved boundary element method for the charge density of a thin electrified plate in $\boldsymbol{R}^3$, Math. Meth. Appl. Scis. **13**, 291-303, 1990.

[4] I. G. Graham, W. Hackbusch and S. A. Sauter. Discrete boundary element methods on general meshes in 3D. Bath Mathematics Preprint 97/19, 1997

[5] I.G. Graham, W. Hackbusch and S.A. Sauter, Hybrid boundary elements: Theory and implementation. Preprint Number 98-6, University of Kiel, Feb. 1998.

[6] W. Hackbusch and S. A. Sauter. On the efficient use of the Galerkin method to solve Fredholm integral equations. Applications of Mathematics, **38**:301–322, 1993.

[7] T. von Petersdorff, Elasticity Problems in Polyhedra-Singularities and Approximation with Boundary Elements, Ph.D. Dissertation, T.H. Darmstadt, 1989.

[8] S. A. Sauter. Cubature techniques for 3D Galerkin BEM, in W. Hackbusch and G. Wittum, editors, BEM: Implementation and Analysis of Advanced Algorithms, Vieweg Verlag, 1996.

[9] S. A. Sauter and A. Krapp On the effect of numerical integration in the Galerkin boundary element method. Numer. Math. **74**, 337-359, 1997.

[10] S.A. Sauter and C. Schwab, Quadrature for $hp-$ Galerkin BEM in 3D, Numer. Math. **78**, 211-258, 1997.

[11] I.H. Sloan, Semidiscrete Galerkin method for piecewise-smooth curves and surfaces, Submitted for publication.

[12] W.L. Wendland, On Galerkin collocation methods for integral equations of elliptic boundary value problems, in "Numerical Treatment of Integral Equations", J. Albrecht and L. Collatz, Eds., ISNM 53, Birkhauser-Verlag, Basel, 1980.